Optimization of Acryloylphenylcarboxamides as Inhibitors of ABCG2 and Comparison with Acryloylphenylcarboxylates

Stefanie Kraege, Katja Stefan, Sebastian C. Köhler, and Michael Wiese*[a]

ABCG2 belongs to the superfamily of ATP binding cassette (ABC) proteins and is associated with the limited success of anticancer chemotherapy, given its responsibility for the cross-resistance of tumor cells, known as multidrug resistance (MDR). Several classes of ABCG2 inhibitors were developed for increasing the efficacy of chemotherapy. A series of chalcones coupled to an additional aromatic residue was synthesized and investigated for their inhibition of ABC transporters. In our previous work we determined the preferred position of the linker on the A-ring to be *ortho*, and found several substitution patterns at the additional ring that improved potency. In this study we investigated whether a methoxy group that improved the inhibitory activity of chalcones would also be beneficial for the acryloylphenylcarboxamide scaffold. Indeed, this modification led to highly potent ABCG2 inhibitors. To support the hypothesis of a beneficial effect of the amide linker, six acryloylphenylcarboxylates were synthesized and investigated for their inhibitory activity. Replacement of the amide linker with an ester group resulted in decreased inhibition. Molecular modeling showed that the conformational preference of both series differs, thereby explaining the positive effect of the amide linker. Several compounds were characterized in detail by investigating their intrinsic cytotoxicity and capacity to reverse MDR in MTT assays and their effect on vanadate-sensitive ATPase activity.

Introduction

Chemotherapy often fails due to tumor cell cross-resistance to anticancer drugs. Various mechanisms behind multidrug resistance (MDR) have been postulated and often lead to the same consequence: the intracellular decrease of cytotoxic agents. One extensively studied mechanism generating MDR is the overexpression of membrane efflux pumps belonging to the family of ATP binding cassette (ABC) proteins.[1,2] These pumps catalyze the transport of substrates across membranes against their concentration gradient by ATP hydrolysis. They can behave as importers, bringing nutrients into the cell, or as exporters, transferring toxins, drugs, and lipids out of cells. Present in both prokaryotes and eukaryotes, these transport proteins perform diverse functions.[3–5] While export proteins are found in both types of organism, import proteins appear to exist exclusively in prokaryotes.

The 48 human ABC proteins are divided into seven subfamilies: ABCA through ABCG.[6] ABC transporters possess a characteristic architecture that minimally consists of four domains to generate a functional unit: two transmembrane domains (TMDs) embedded in the membrane and two nucleotide binding domains (NBDs) located in the cytoplasm that are responsible for the hydrolysis of ATP to ADP and P_i.[7] Three ABC transporters are well-recognized to play a major role in the emergence of MDR: ABCB1 (P-glycoprotein, P-gp), ABCC1 (multidrug resistance-associated protein 1, MRP1), and ABCG2 (breast cancer resistance protein, BCRP).[8–10] A common strategy to overcome MDR is the development of potent and selective inhibitors of ABCB1, ABCC1, and ABCG2. Blocking the efflux mechanism should result in higher intracellular accumulation of anticancer drugs and an increased efficiency of chemotherapy.

ABCG2 is the most recently characterized ABC transporter implicated in MDR and was first discovered in 1998.[10,11] While ABCB1 and ABCC1 act as full transporters, ABCG2 was described as a half transporter containing only one TMD and NBD, requiring at least dimerization to function as an efflux pump.[12,13] It was recently proposed that the functional transporter is formed by tetramerization.[14] The protein is present in various organs with a barrier function, and is overexpressed in several tumor cells as well.[15] The structural diversity of substrates extends from anticancer drugs such as mitoxantrone over tyrosine kinase inhibitors to fluorescent dyes such as Hoechst 33342.[16] Fumitremorgin C (FTC) was the first identified selective inhibitor of ABCG2, completely reversing mitoxantrone resistance in ABCG2 cells. This natural product was isolated from *Aspergillus fumigatus*, but turned out to be clinically useless owing to its neurotoxicity.[17–19] Based on the indolyl diketopiperazine moiety, several structurally related analogues were developed, especially the less toxic and more potent inhibitor Ko143, the clinical use of which is limited by metabolic instability due to its Boc-ester group.[20,21] Furthermore, new specific and highly potent ABCG2 inhibitors were developed

[a] S. Kraege, K. Stefan, S. C. Köhler, Prof. Dr. M. Wiese
     Pharmaceutical Chemistry II, Pharmaceutical Institute, University of Bonn,
     An der Immenburg 4, 53121 Bonn (Germany)
     E-mail: mwiese@uni-bonn.de

from other structural classes such as quinazolines, chromones, and chalcones.[22–24]

Amide groups are present in a number of ABCG2 inhibitors such as Ko143 and its derivatives, and the dual ABCB1 and ABCG2 inhibitors elacridar and tariquidar. As reported in our previous study, we combined the chalcone scaffold with an additional aromatic residue by an amide linker leading to acryloylphenylcarboxamides as new class of ABCG2 inhibitors including structural modifications at positions 2′, 3′, and 4′ on ring A and positions 3 and 4 on ring B of the chalcone.[25] We examined the best position of the amide linker and found the *ortho* position to be highly preferable over *para* and *meta*. On ring B of the chalcone, a dimethoxy substitution was beneficial. The most potent compound, bearing a 2-thienyl substitution connected to the chalcone moiety, had an IC$_{50}$ value in the high nanomolar range and was found to be almost exclusively selective toward ABCG2 and also nontoxic.

To optimize the acryloylphenylcarboxamide moiety, we investigated whether a 4′-methoxy group would further improve inhibitory activity, as this substituent had been proven beneficial in the case of simple chalcones.[22] For this purpose, we synthesized 20 methoxy-substituted acryloylphenylcarboxamides. To investigate the contribution of the amide linker, it was replaced by an ester group in six acryloylphenylcarboxylates. All new compounds were tested for their inhibitory potencies toward ABCG2 by Hoechst 33342 assay using MDCK II BCRP cells. Furthermore, ABCG2 selectivity was determined by screening for ABCB1 and ABCC1 inhibition using the calcein AM assay. To determine the feasibility of these compounds in future in vivo studies, their intrinsic cytotoxicity was examined by MTT assay.

Results and Discussion

Chemistry

The synthesis of target compounds **7**–**32** is illustrated in Scheme 1. For 4′-methoxy-substituted acryloylphenylcarboxamides, the synthesis starts with a Houben–Hoesch reaction (a special Friedel–Craft acylation) to yield 4′-methoxy-2′-aminoacetophenone.[26] For this purpose, 3-anisidine was treated with acetonitrile in the presence of boron trichloride and aluminum trichloride. All other acetophenones were commercially available. In the following step, a Claisen–Schmidt condensation between the ketone and variously substituted benzaldehydes gave the key intermediate chalcones. Afterward a solution of chalcone and selected acid chloride in tetrahydrofuran was stirred overnight at room temperature in the presence of triethylamine to form the amide linker. The title compounds were characterized by NMR spectroscopy and their purity was confirmed by elemental analysis.
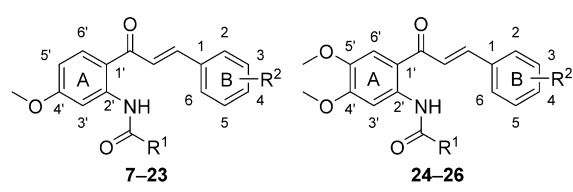
Biological investigations

Inhibition of ABCG2

The inhibitory activity of the compounds toward ABCG2 was investigated by Hoechst 33342 assay using the MDCK II BCRP cell line. The fluorescent dye Hoechst 33342 is a bisbenzimidazole derivative and was found to be transported by ABCG2.[27] This assay was performed as previously described with minor modifications.[28–30] Calculated IC$_{50}$ values of methoxy-substituted acryloylphenylcarboxamides **7**–**26** are listed in Table 1, and
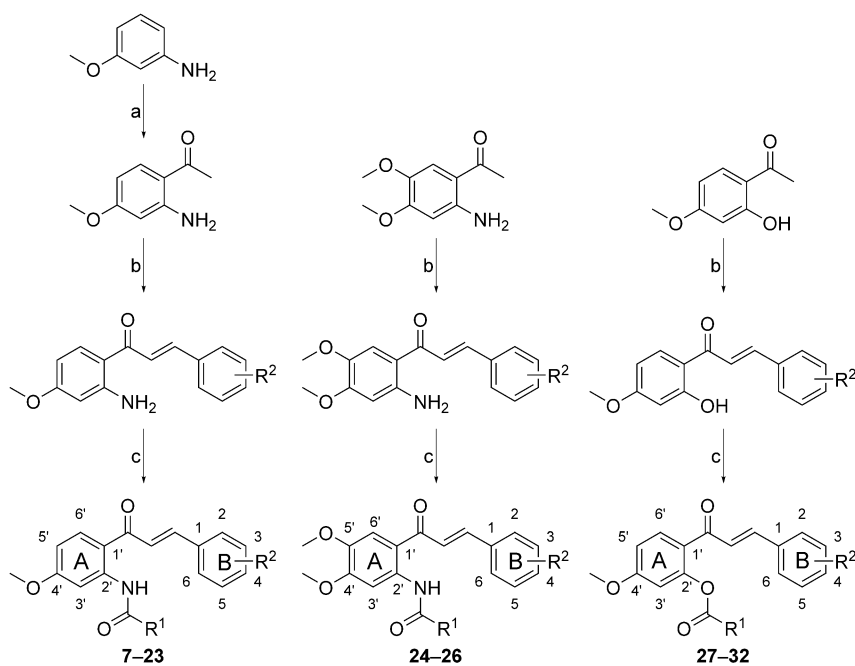
Scheme 1. General synthesis of the methoxy-substituted acryloylphenylcarboxamides and acryloylphenylcarboxylates **7**–**32**. *Reagents and conditions*: a) BCl$_3$, AlCl$_3$, acetonitrile, CH$_2$Cl$_2$, 0 °C, reflux, 80 °C, 20 h, cooling to 0 °C, 2 N HCl, stirring 30 min at 80 °C; b) substituted benzaldehyde, LiOH, MeOH, ultrasonic bath, 4–8 h; c) acid chloride, triethylamine, THF, RT, overnight.
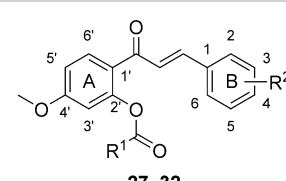
↖↖ **These are not the final page numbers!**

Table 1. Inhibitory activities of methoxy-substituted acryloylphenylcarboxamides (**7–26**) against ABCG2 determined by Hoechst 33342 assay using MDCK II BCRP cells.

Compd	R^1	R^2	IC$_{50}$ [μm][a]
7	phenyl	3,4-dimethoxy	0.219 ± 0.033
8	3-chlorophenyl	3,4-dimethoxy	–[b]
9	2-chlorophenyl	3,4-dimethoxy	0.660 ± 0.088
10	3-bromophenyl	3,4-dimethoxy	–[b]
11	2-methoxyphenyl	3,4-dimethoxy	0.285 ± 0.033
12	3-pyridyl	3,4-dimethoxy	1.17 ± 0.05
13	2-pyridyl	3,4-dimethoxy	1.36 ± 0.16
14	1-naphthyl	3,4-dimethoxy	0.422 ± 0.083
15	3-quinolinyl	3,4-dimethoxy	–[b]
16	2-thienyl	3,4-dimethoxy	0.320 ± 0.032
17	2-furanyl	3,4-dimethoxy	0.714 ± 0.061
18	2-thiazyl	3,4-dimethoxy	1.01 ± 0.13
19	phenyl	3,5-dimethoxy	0.292 ± 0.030
20	2-methoxyphenyl	3,5-dimethoxy	0.595 ± 0.062
21	2-chlorophenyl	3,5-dimethoxy	0.358 ± 0.025
22	2-thienyl	3,5-dimethoxy	0.268 ± 0.058[c]
23	1-naphthyl	3,5-dimethoxy	0.359 ± 0.076[c]
24	phenyl	3,4-dimethoxy	0.754 ± 0.105
25	2-methoxyphenyl	3,4-dimethoxy	0.832 ± 0.111
26	2-thienyl	3,4-dimethoxy	–[b]

[a] Values are the mean ± SD of at least three independent measurements. [b] Compound was too insoluble and precipitated. [c] Maximum inhibition reached decreased to 60–70% relative to the standard Ko143 (100%).

Table 2. Inhibitory potencies of synthesized acryloylphenylcarboxylates **27–32** determined by Hoechst 33342 assay using MDCK II BCRP cells and comparison with their carboxamide analogues.

Compd	R^1	R^2	IC$_{50}$ ± SD [μm][a]	Amide	IC$_{50}$ [μm][a]
27	phenyl	3,4-dimethoxy	0.879 ± 0.125	7	0.219
28	2-thienyl	3,4-dimethoxy	2.08 ± 0.35	16	0.320
29	2-methoxyphenyl	3,4-dimethoxy	1.44 ± 0.17	11	0.285
30	phenyl	3,5-dimethoxy	1.09 ± 0.20	19	0.292
31	2-thienyl	3,5-dimethoxy	0.865 ± 0.169	22	0.268
32	2-methoxyphenyl	3,5-dimethoxy	1.70 ± 0.21	20	0.595

[a] Values were determined from at least three independent experiments.

IC$_{50}$ values of acryloylphenylcarboxylates **27–32** are provided in Table 2.

According to their substitution pattern, the methoxy-substituted acryloylphenylcarboxamides can be divided into three different series. The first series (**7–18**) of 4′-methoxy-substituted acryloylphenylcarboxamides contain a 3,4-dimethoxy substitution on ring B of the chalcone, and varies in the R^1 group on the amide linker. Compound **7**, bearing an unsubstituted phenyl ring, turned out to be the most potent ABCG2 inhibitor, with an IC$_{50}$ value of 0.219 μm. Therefore, it is the most promising derivative of all investigated acryloylphenylcarboxamides. The halogen-substituted compounds **8** (3-chlorophenyl) and **10** (3-bromophenyl) could not be examined for their inhibitory activity due to poor solubility. However, moving the chloro substituent to the *ortho* position yielded a compound with good activity (**9**: IC$_{50}$ = 0.660 μm). Roughly similar inhibitory potencies to that of the best compound **7** were reached by representatives bearing a 2-methoxyphenyl (**11**: IC$_{50}$ = 0.285 μm) or 2-thienyl residue (**16**: IC$_{50}$ = 0.320 μm). Our previous studies demonstrated the benefit of thienyl substitution, showing IC$_{50}$ values in the sub-micromolar range. To examine the necessity of a sulfur atom within the five-membered ring system, we synthesized two further derivatives by replacing the sulfur with oxygen or by adding nitrogen. In comparison, compound **17** containing a 2-furanyl group (IC$_{50}$ = 0.714 μm) and **18** with a 2-thiazyl group (IC$_{50}$ = 1.01 μm) showed good but lower activity in ABCG2 inhibition. For the phenyl (**7**) and these three five-membered ring compounds (**16–18**), there is a very good correlation between pIC$_{50}$ and log *P* (*R*^{2} = 0.90) pointing to partitioning as an additional contribution. The pyridyl derivatives **12** (*meta*: IC$_{50}$ = 1.17 μm) and **13** (*ortho*: IC$_{50}$ = 1.36 μm) were less potent than the unsubstituted phenyl derivative. In summary, the synthesis of 4′-methoxy-substituted acryloylphenylcarboxamides resulted in highly potent ABCG2 inhibitors.

In the second series of 4′-methoxy-substituted acryloylphenylcarboxamides (**19–23**) we replaced the 3,4-dimethoxy substitution with 3,5-dimethoxy groups. Therefor, five different derivatives were synthesized containing amide residues that had been proven to yield highly potent derivatives in the 3,4-dimethoxy series. Compound **19** (phenyl: IC$_{50}$ = 0.292 μm) showed similar and **20** (2-methoxyphenyl: IC$_{50}$ = 0.595 μm) slightly decreased activity relative to their counterparts from the first series. In contrast, compound **21**, bearing a 2-chlorophenyl group, reached ~2-fold higher inhibitory potency toward ABCG2 than the counterpart with an IC$_{50}$ value of 0.358 μm. Both compounds **22** (IC$_{50}$ = 0.268 μm) and **23** (IC$_{50}$ = 0.359 μm) showed similar activity as well. However, both representatives showed decreased fluorescence intensity (60–70%) relative to the standard (Ko143: 100%).

Members of the third series of acryloylphenylcarboxamides (**24–26**) bear a 4′,5′-dimethoxy substitution instead of 4′-methoxy on ring A of the chalcone moiety. Three derivatives were synthesized to evaluate the influence of an additional methoxy group. Compound **24** (phenyl: IC$_{50}$ = 0.714 μm) und **25** (2-methoxyphenyl: IC$_{50}$ = 0.832 μm) showed good inhibitory activity, but were less potent than in the other two series. For the 2-thienyl derivative **26**, no IC$_{50}$ value could be determined due to low solubility.

To investigate the importance of the amide linker a series of six acryloylphenylcarboxylates was synthesized, containing an ester function instead of the amide group. All investigated compounds possess a 4'-methoxy substituent on ring A and contain either a 3,4-dimethoxy or 3,5-dimethoxy substitution on ring B of the chalcone substructure. In relation to the inhibitory effect toward ABCG2 there was no significant difference between these two groups. A comparison of the acryloylphenylcarboxylates with their carboxamide analogues showed 3- to 6-fold lower IC_{50} values for the latter group, pointing to a beneficial effect of the amide function for inhibitory activity. Priority ranking within the 3,4-dimethoxy (27–29) and 3,5-dimethoxy series (30–32) consistently demonstrated the same effect on activity as obtained for the acryloylphenylcarboxamides. In the 3,4-dimethoxy series the phenyl derivative (27: $IC_{50}=0.879\ \mu M$) demonstrated the best inhibitory potency, followed by 2-methoxyphenyl (29: $IC_{50}=1.44\ \mu M$) and finally ending with 2-thienyl (28: $IC_{50}=2.08\ \mu M$). In the 3,5-dimethoxy series compound 31 (thienyl, $IC_{50}=0.865\ \mu M$) showed the highest activity followed by the phenyl and 2-methoxyphenyl derivatives.

The decreased activity despite higher lipophilicity of the esters could be due to different preferred conformations. To investigate this possibility, we performed conformational analysis of compounds 7 and 27 independently using the low-mode molecular dynamics method in MOE.[31] The low-mode search method generates conformations using a short run of molecular dynamics at constant temperature (300 K) followed by an all-atom energy minimization. The method was initially intended for large and complex structures such as macrocycles and

protein loops, but it was found to be very efficient for detailed small-molecule analysis as well. It generates a table with a number of conformations ranked by potential energy. For compound 7 a planar arrangement of the chalcone carbonyl and the amide group was observed in all low-energy conformations. The planar conformation is stabilized by an intramolecular hydrogen bond between the amide linker and the carbonyl oxygen atom as shown in Figure 1A, while in the case of the esters electrostatic repulsion leads to a V-shaped conformation as seen in Figure 1B. In Figure 1C the overlay of both compounds is shown for better comparison. We further investigated whether the compounds could be better overlaid performing a fully flexible alignment. This yielded a perfect match of the molecules as shown in Figure 1D; however, the potential energies of both compounds were 9.1 (7) and 6.8 kcal mol^{-1} (27) above the global minimum found in the conformational search, making this superposition rather unlikely. Thus, it could be concluded that both series of derivatives adopt different conformations in solution and upon binding.

A graphical description of structural features influencing the activity of acryloylphenylcarboxamides is given in Figure 2. During the process of optimization in this new class of ABCG2 inhibitors we established four important facts related to the acryloylphenylcarboxamide moiety and thus for activity: 1) An amide linker in the ortho position of the chalcone moiety, 2) 4'-methoxy substitution on ring A, 3) dimethoxy substitution on ring B, and especially 4) phenyl or 2-thienyl substitution at the amide substructure increased potency.
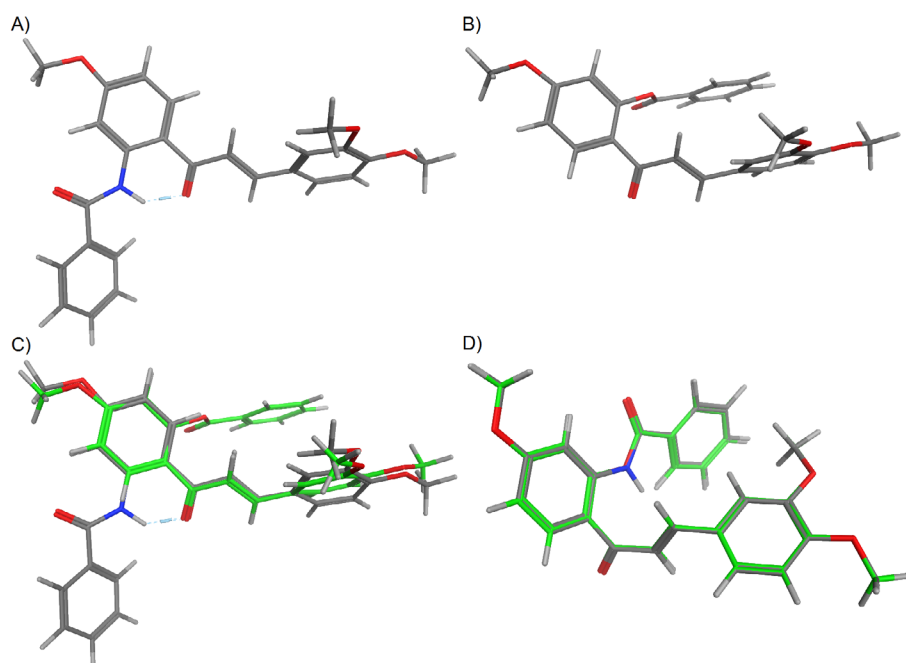

Figure 1. Lowest-energy conformations of A) compound 7 with an amide linker and B) compound 27 containing an ester group. C) Both conformations are superimposed for better comparison with compound 27, shown in green. D) The perfect match from a fully flexible alignment. However, the potential energies of both molecules are 9.1 (7) and 6.8 kcal mol^{-1} (27) above the global minima shown in panels A)–C), making these conformations unlikely. Note that the hydrogen bond between the amide group and the carbonyl oxygen atom is missing, which is present in the low-energy conformations of compound 7.

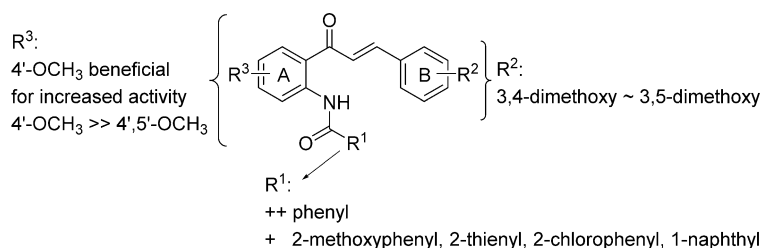↖↖ **These are not the final page numbers!**

Figure 2. Structural features of the methoxy-substituted acryloylphenylcarboxamides as potent ABCG2 inhibitors. +: good activity, + +: very high activity.

Determination of ABCB1 and ABCC1 inhibition

For extensive characterization of methoxy-substituted acryloyl-phenylcarboxamides and acryloylphenylcarboxylates, calcein AM assay was performed as previously described with minor modifications.[24 32,33] This provides insight into the behavior toward the two other major ABC transporters, ABCB1 and ABCC1. For this purpose, ABCB1-overexpressing A2780 adr cells and ABCC1-overexpressing H69 AR cells were used. Cyclosporine A (CsA), a well-known inhibitor of both ABC transporters, served as standard. In the first instance, all compounds were screened for their ability to inhibit ABCB1 and ABCC1 at a fixed concentration of 10 μM. For comparison, the effect of inhibition was calculated as percentage response at 10 μM relative to CsA (10 μM, 100% inhibition). The resulting data are shown in Figures 3 and 4. As can be seen from the figures some compounds showed notable inhibition of ABCB1 (Figure 3), whereas for ABCC1 almost no inhibitory effect was observed (Figure 4).

For compounds showing an inhibition response $\geq 25\%$, IC_{50} values were determined (Table 3). Except for compounds **7**, **11**, **12**, **13**, **17**, and **20**, no significant affinity ($\leq 25\%$) toward ABCB1 was observed in the series of 4'-methoxy-substituted acryloylphenylcarboxamides. It is known that methoxy substitution plays a major role in ABCB1 affinity.[34] Both the number and position of these residues affect the inhibitory potential. Compound **11**, bearing an additional 2-methoxy group at the
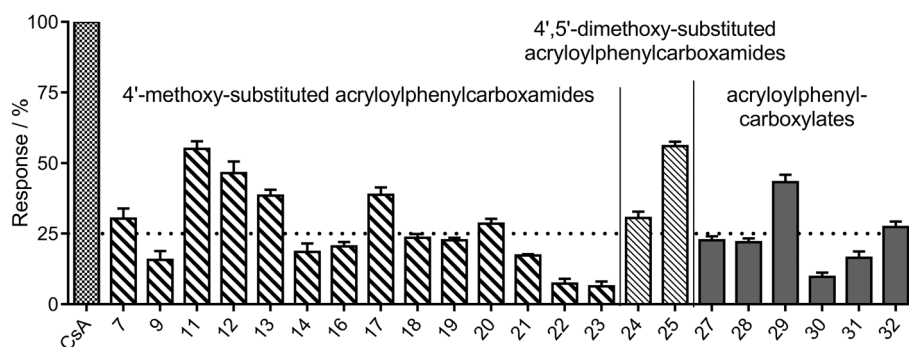

Figure 3. Effect of acryloylphenylcarboxamides **7–26** and analogues **27–32** on the calcein AM assay in the ABCB1-overexpressing A2780 adr cell line at a concentration of 10 μM. Data were obtained from three independent experiments and are given as percentage of the positive control (cyclosporine A, CsA, 10 μM).

Figure 4. Effect of acryloylphenylcarboxamides **7–23** and analogues **27–32** on the calcein AM assay in the ABCC1-overexpressing H69 AR cell line at a concentration of 10 μM. Data were obtained from three independent experiments and are given as percentage of the positive control (cyclosporine A, CsA, 10 μM).
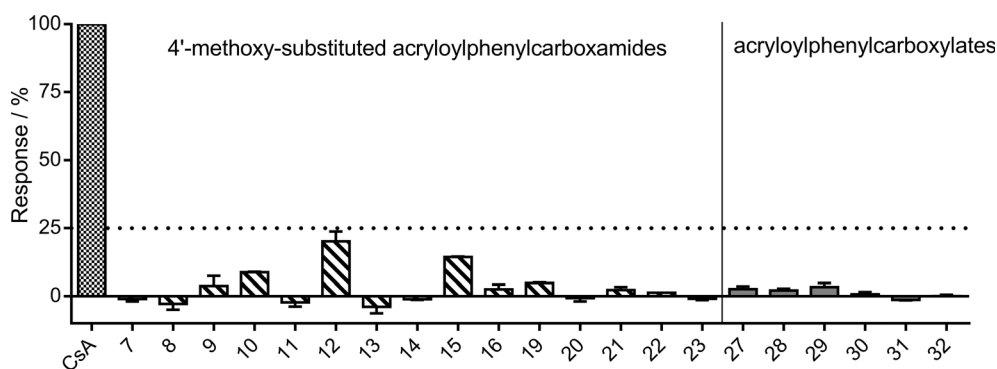
These are not the final page numbers! ↗↗

Table 3. Inhibitory activities of selected compounds against ABCB1-over-expressing A2780adr cells determined by calcein AM assay.

Compd	IC_{50} [μM][a]	I_{max} [%][a,b]
7	1.13 ± 0.10	32 ± 9
11	0.848 ± 0.130	58 ± 5
12	1.37 ± 0.10	41 ± 2
13	0.777 ± 0.066	36 ± 2
17	1.64 ± 0.26	39 ± 6
20	0.250 ± 0.032	29 ± 4
24	3.51 ± 0.44	31 ± 4
25	1.45 ± 0.03	57 ± 6
29	2.16 ± 0.32	40 ± 4
32	2.0 ± 0.26	27 ± 4
CsA	0.862 ± 0.059	100

[a] Data are the mean ± SD of at least three independent measurements. [b] Maximum inhibition relative to the standard inhibitor cyclosporine A (CsA; $I_{max} = 100\%$).

Table 4. Intrinsic cytotoxicity of selected methoxy-substituted acryloyl-phenylcarboxamides determined by MTT assay using MDCK II BCRP and MDCK II wild-type cells.

Compd	IC_{50} [μM][a,b]	GI_{50} [μM][a,c]		TR[d]
		BCRP	wild-type	
7	0.219	78 ± 9	80 ± 9	356
11	0.285	21 ± 4	18 ± 3	74
16	0.320	21 ± 2	17 ± 2	66
19	0.292	22 ± 4	17 ± 3	75
22	0.268	18 ± 3	18 ± 2	67

[a] Compounds were investigated up to a concentration of 100 μM for 72 h. [b] Hoechst 33342 assay. [c] Values are the mean ± SD of at least three independent experiments. [d] Therapeutic ratio: $GI_{50\,BCRP}/IC_{50}$.

phenylcarboxamide, showed the highest effect toward ABCB1, with a maximal response of 58% inhibition and an IC_{50} value of 0.848 μM. The pyridyl derivatives **12** ($IC_{50} = 1.37$ μM) and **13** ($IC_{50} = 0.777$ μM) were found to possess similar potency, but with reduced maximal response. Compound **20** had the lowest IC_{50} value of 0.250 μM. However, it only reached a maximum inhibition of 29% relative to CsA.

The acryloylphenylcarboxylates with an ester linker behaved similar to the amides. Only compounds **29** ($IC_{50} = 2.16$ μM) and **32** ($IC_{50} = 2.0$ μM) bearing a 2-methoxyphenyl group showed noteworthy affinity toward ABCB1.

MTT assay

The yellow tetrazole MTT (methylthiazolyldiphenyltetrazolium bromide or 3-(4,5-dimethythiazol-2-yl)-2,5-diphenyltetrazolium bromide) is reduced to purple formazan in living cells by mitochondrial reductases. The formation of formazan depends on the cellular metabolic activity due to NAD(P)H flux and is therefore specific for living cells. This property can be used for the determination of cytotoxic effects. Formed formazan crystals that are insoluble in water can be dissolved in DMSO and measured spectrophotometrically.

MTT cytotoxicity assays were performed for selected 4′-methoxy-substituted acryloylphenylcarboxamides using MDCK II BCRP and MDCK II wild-type cells.[32] The compounds were investigated up to a final concentration of 100 μM. Obtained GI_{50} values are summarized in Table 4. Furthermore, the therapeutic ratio was calculated from the IC_{50} values obtained in the Hoechst 33342 assay and the GI_{50} values, which is an important parameter for further in vivo studies.[24] Among the investigated modulators, compound **7**, which is most potent in the Hoechst 33342 assay, showed only very low intrinsic cytotoxicity with a GI_{50} value of 78 μM (concentration–response curve is given in Figure 5), yielding the highest therapeutic ratio. The other derivatives possessed 4-fold higher cytotoxicity with GI_{50} values of ~20 μM. However, these concentrations are much higher than the IC_{50} values for ABCG2 inhibition.
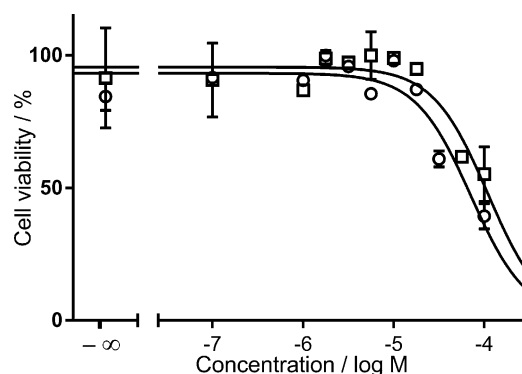

Figure 5. Representative concentration–response curve of compound **7** obtained in the MTT assay using MDCK II BCRP (○) and MDCK II wild-type cells (□). The compound was investigated up to a final concentration of 100 μM after 72 h incubation time ($GI_{50} = 78$ μM). Data are given as mean ± SD.

The MTT assay was also used to determine the ability of 4′-methoxy-substituted acryloylphenylcarboxamides to sensitize MDCK II BCRP cells toward cytotoxic agents. Therefore, the cytotoxicity of the cytostatic SN-38 (active metabolite of irinotecan) was investigated in MDCK II cells, in the presence or absence of selected compounds (Table 5).

Representative dose–response curves of compound **7** (Figure 6) illustrate the shift of SN-38 cytotoxicity in MDCK II BCRP cells toward the viability of MDCK wild-type cells, showing the capacity of compound **7** to reverse MDR in ABCG2-overexpressing cells.

Table 5. The ability of selected compounds to reverse resistance toward SN-38 in MDCK II BCRP and MDCK II wild-type cells.

Compd	GI_{50} [μM][a]			
	BCRP	BCRP + 0.1 μM inhibitor	BCRP + 0.5 μM inhibitor	wild-type
7	2.45 ± 0.24	0.732 ± 0.043	0.356 ± 0.055	0.209 ± 0.028
11	2.52 ± 0.34	1.01 ± 0.13	0.428 ± 0.059	0.211 ± 0.034
16	2.88 ± 0.41	0.684 ± 0.104	0.352 ± 0.035	0.215 ± 0.032
22	2.37 ± 0.31	0.586 ± 0.092	0.376 ± 0.015	0.225 ± 0.042
average	2.56 ± 0.23			0.215 ± 0.007

[a] Values are the mean ± SD of at least three independent experiments.
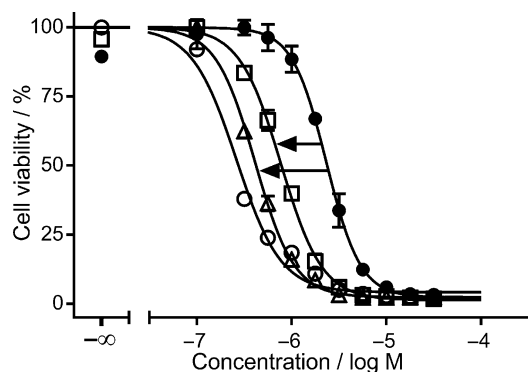
↖↖ **These are not the final page numbers!**

Figure 6. Representative dose–response curves of SN-38 cytotoxicity obtained in MTT assay using MDCK II BCRP and MDCK II wild-type cells. Arrows illustrate the dose-dependent sensitization of MDCK II BCRP cells by compound **7** toward SN-38. MDCK II wild-type cells+SN-38 without inhibitor (positive control: ○), SN-38+0.1 μM **7**: □, SN-38+0.5 μM **7** and MDCK II BCRP cells: △, MDCK II BCRP cells+SN-38 without inhibitor: ●.

Vanadate-sensitive ATPase activity assay

For the characterization of acryloylphenylcarboxamides in greater detail, we examined their effect at a concentration of 1 μM on the vanadate-sensitive ATPase activity using ABCG2-containing cell membranes from Sf9 cells infected with an ABCG2-containing baculovirus. The assay was performed as described previously.[35] All investigated compounds showed stimulation of ATPase activity relative to basal activity (Figure 7). However, there are clear differences between the four series. The first two series vary by the substitution at position 4′ of the chalcone moiety and showed similar ATPase activity. In comparison, derivatives from series three (**19** and **22**) bearing a dimethoxy substitution in position 3,5 instead of 3,4 on ring B demonstrated a high increase of stimulation beyond the level of the well-known activator quercetin. The two representatives from the last series, containing the 4,5-dimethoxy-sub-

stituted acryloylphenylcarboxamide scaffold (**24** and **26**), resulted in slightly less stimulation but still higher than the first and second series. This result highlights the structural dependence of ATPase stimulation by the presence and position of methoxy groups. Our previous studies on quinazoline-chalcones demonstrated the influence of methoxy substitution in relation to a stimulating effect on ATPase activity, without indication of being a substrate.[35] In the MTT cytotoxicity assay no significant difference between ABCG2-transfected and control cells was observed, proving that the substances are not effectively transported by ABCG2. Although acryloylphenylcarboxamides stimulate vanadate-sensitive ATPase activity, they were found to be inhibitors of ABCG2.

For flavonoids, the biosynthetic successors of chalcones, numerous docking and 3D QSAR studies demonstrated that they target the NBD of ABCB1.[36–38] With regard to ABCG2 no comprehensive studies have been published. Chalcones have not been investigated that intensively, but they were shown to interact with the NBDs of ABCB1 by Bois et al.[39,40] Though nothing definite is known for ABCG2, but due to the highly conserved NBD structures, an analogous interaction can be assumed, as for flavonoids. This is substantiated by the finding that chalcones can interact with the ATP binding site of tyrosine kinases.[41,42] However, more and detailed investigations are necessary to prove the mode of interaction of these compounds with ABCG2.

Conclusions

In the present work 20 new acryloylphenylcarboxamides and six acryloylphenylcarboxylates were synthesized and investigated for their influence on ABC transporters, especially ABCG2. Four important conclusions could be drawn by analyzing the structure–activity relationships.

First, a 4′-methoxy substitution on ring A of the chalcone moiety leads to an increased inhibitory activity toward ABCG2
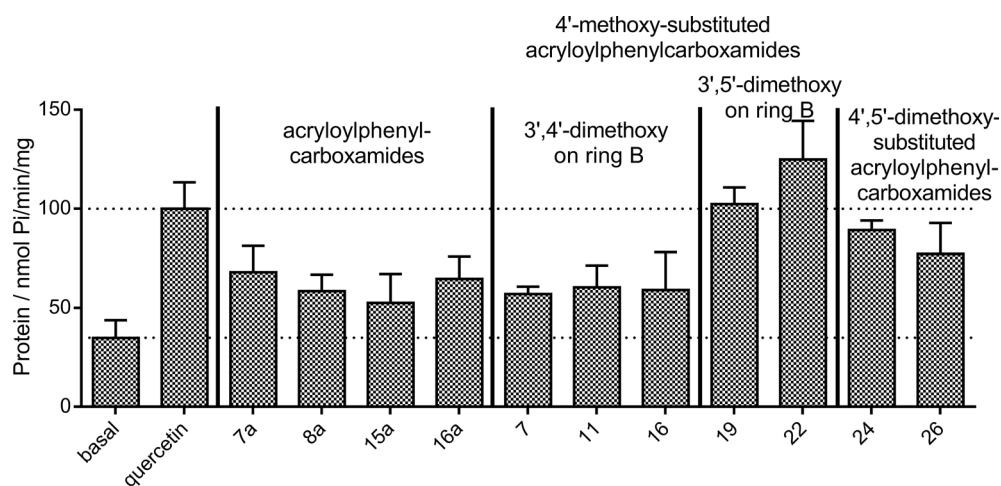

Figure 7. Vanadate-sensitive ATPase activity of selected acryloylphenylcarboxamides in isolated ABCG2 containing Sf9 membranes at a fixed concentration of 1 μM. Data were obtained from three independent experiments and are depicted as mean±SD. Compounds **7a**, **8a**, **15a** and **16a** correspond structurally to compounds **7**, **8**, **15**, **16** but lack the 4′-methoxy group. These compounds were synthesized previously (corresponding compound numbers in Kraege et al.: **26**, **27**, **33**, **37**).[25]

These are not the final page numbers! ↗↗

and was therefore characterized as beneficial structural feature. In comparison, the 4′,5′-dimethoxy substitution resulted in slightly decreased potencies of the compounds. Furthermore, we observed only weak affinity toward ABCB1, except for compounds bearing an additional methoxy group at the benzamide. The data indicate that most of the investigated derivatives are almost exclusively selective ABCG2 inhibitors. There was no significant difference between chalcones substituted with 3,4- or 3,5-dimethoxy groups on ring B, as well as comparable 4′-methoxy-substituted acryloylphenylcarboxamides and benzoates. As expected, an increased number of methoxy groups led to increased ABCB1 affinity.

Second, for the substitution pattern on ring B of the chalcone moiety, 3,4-dimethoxy groups were confirmed as the most efficient pattern among those investigated. While 3,5-dimethoxy groups partially yielded a slightly increased potency (**9** versus **21** and **14** versus **23**), the maximum inhibition was less.

Third, we investigated the influence of an amide linker by replacing it with an ester function. The acryloylphenylcarboxylates showed moderate but decreased inhibitory effects toward ABCG2. This might be the result of lost donor–acceptor behavior by switching nitrogen to oxygen and/or the different preferred conformation. As before, shifting one methoxy group to the second *meta* position on ring B of the chalcone resulted in comparable IC$_{50}$ values.

Fourth, we demonstrated the effect of methoxy groups on the vanadate-sensitive ATPase activity. All investigated compounds stimulated the ATPase above the level of basal activity, but to various magnitudes. While the variation of methoxy substitution on ring A had no relevant consequences, the exchange of 3,4-dimethoxy by 3,5 dimethoxy groups on ring B resulted in a large increase in stimulation of ATPase activity (compounds **19** and **22**), actually higher than reached by quercetin, a well-known substrate of ABCG2. Despite the activation of ATPase activity, the acryloylphenylcarboxamides were found to be inhibitors of ABCG2.

In conclusion, within this new series of acryloylphenylcarboxamides several highly potent and nontoxic ABCG2 inhibitors were identified, showing only weak affinity toward ABCB1 and ABCC1. Compound **7** turned out to be the most active derivative, containing the most important structural features for high potency: *ortho* position of the amide linker, 4′-methoxy substitution on ring A, 3,4-dimethoxy groups on ring B, and an unsubstituted phenyl ring as additional residue.

Experimental Section

Chemistry

Materials: Reagents were purchased from Acros Organics, Sigma–Aldrich, or Alfa Aesar and were used without further purification. For examination of reaction progress, thin-layer chromatography (TLC) was performed. Aluminum sheets coated with silica gel 60 F$_{254}$ (Merck) and cyclohexane/ethyl acetate (2:8) as eluent was used. Melting points were measured on a Stuart melting point apparatus model SMP3 (Barloworld Scientific Limited Stone, Staffordshire, ST15 0SA, UK). All structures of target compounds were approved by NMR. ^{1}H NMR and ^{13}C NMR spectra were processed on a Bruker Advance 500 MHz NMR spectrometer at 500 MHz (^{1}H) or 126 MHz (^{13}C), or a Bruker Advance 600 MHz (^{1}H, 600 MHz/^{13}C, 151 MHz) NMR spectrometer. Exclusively [D$_6$]DMSO was used as solvent at 303 K. The chemical shifts were reported as parts per million [ppm] relative to [D$_6$]DMSO, ^{1}H, $\delta = 2.54$ ppm; ^{13}C, $\delta = 40.45$ ppm. Coupling constants (*J*) are given in Hertz, and spin multiplicities are reported as s (singlet), d (doublet), doublet of doublets (dd), triplet of doublets (td), t (triplet), doublet of triplets (dt), q (quartet), and m (multiplet). ^{13}C NMR signals were assigned with the aid of distortionless enhancement by polarization transfer (DEPT) and attached proton test (APT). The purity of all target compounds was determined to be > 95 % by elemental analyses on a Vario EL V24 CHN elemental analyzer; all determined values were within ± 0.4 % of the theoretical values, if not indicated otherwise. Spectral data of all compounds together with other physicochemical characteristics are given in the Supporting Information.

General procedure for the preparation of 1-(2-amino-4-methoxyphenyl)ethan-1-one. A solution of 3-methoxyaniline (21.48 mmol) in 15 mL 1,2-dichloroethane was added to a solution of boron trichloride (23.63 mmol) in dichloromethane at 0 °C. Aluminum chloride (23.63 mmol) and acetonitrile (21.48 mmol) were added, and the mixture was held at reflux at 80 °C for 20 h. After completion of the reaction, the mixture was cooled to 0 °C, and 2 N HCl was added and then stirred for 30 min at 80 °C. The solution was extracted with dichloromethane and the organic layer washed with 1 N NaOH and brine. After drying over anhydrous MgSO$_4$, the solvent was evaporated under reduced pressure to yield the product.

1-(2-amino-4-methoxyphenyl)ethan-1-one (1). The title compound was synthesized from 3-methoxyaniline and acetonitrile to yield white crystals (39 %).

General procedure for the preparation of substituted chalcones. Chalcones **2–6** were synthesized by Claisen–Schmitt condensation. A mixture of selected aminoacetophenone (1 equiv) or 2′-hydroxy-4′-methoxyacetophenone and variously substituted benzaldehyde (1 equiv) and LiOH (7 equiv) as base catalyst in 25 mL methanol were treated in an ultrasonic bath for 4–6 h. After the reaction was complete the mixture was poured onto crushed ice. During the acidification with diluted HCl precipitation of the compounds occurred. The precipitate was filtered off and washed with water. The obtained solid was recrystallized from EtOH/H$_2$O (1:1).

(*E*)-1-(2-amino-4-methoxyphenyl)-3-(3,4-dimethoxyphenyl)prop-2-en-1-one (2). The title compound was synthesized from **1** and 3,4-dimethoxybenzaldehyde to yield a yellow solid (79 %).

(*E*)-1-(2-amino-4-methoxyphenyl)-3-(3,5-dimethoxyphenyl)prop-2-en-1-one (3). The title compound was synthesized from **1** and 3,5-dimethoxybenzaldehyde to yield a yellow solid (73 %).

(*E*)-1-(2-amino-4,5-dimethoxyphenyl)-3-(3,4-dimethoxyphenyl)-prop-2-en-1-one (4). The title compound was synthesized from 4′,5′-dimethoxy-2′-aminoacetophenone and 3,4-dimethoxybenzaldehyde to yield an orange solid (50 %).

(*E*)-3-(3,4-dimethoxyphenyl)-1-(2-hydroxy-4-methoxyphenyl)-prop-2-en-1-one (5). The title compound was synthesized from 2′-hydroxy-4′-methoxyacetophenone and 3,4-dimethoxybenzaldehyde to yield a yellow solid (55 %).

(*E*)-3-(3,5-dimethoxyphenyl)-1-(2-hydroxy-4-methoxyphenyl)-prop-2-en-1-one (6). The title compound was synthesized from 2′-hydroxy-4′-methoxyacetophenone and 3,5-dimethoxybenzaldehyde to yield a yellow solid (30 %).

↖↖ These are not the final page numbers!

General procedure for the preparation of substituted acryloylphenylcarboxamides and acryloylphenylcarboxylates. A solution of selected chalcone (0.25 mmol) and substituted acid chloride (0.25 mmol) in 15 mL tetrahydrofuran was treated with an excess of triethylamine. The mixture was stirred overnight at room temperature. After completion of the reaction the precipitated triethylamine hydrochloride was filtered off and the solvent concentrated in vacuo. The obtained oily residue was recrystallized from ethanol.

(*E*)-*N*-(2-(3-(3,4-dimethoxyphenyl)acryloyl)-5-methoxyphenyl)benzamide (7). The title compound was synthesized from **2** and benzoyl chloride to yield a yellow solid (58 %).

(*E*)-3-chloro-*N*-(2-(3-(3,4-dimethoxyphenyl)acryloyl)-5-methoxyphenyl)benzamide (8). The title compound was synthesized from **2** and 3-chlorobenzoyl chloride to yield a yellow solid (35 %).

(*E*)-2-chloro-*N*-(2-(3-(3,4-dimethoxyphenyl)acryloyl)-5-methoxyphenyl)-benzamide (9). The title compound was synthesized from **2** and 2-chlorobenzoyl chloride to yield a yellow solid (33 %).

(*E*)-3-bromo-*N*-(2-(3-(3,4-dimethoxyphenyl)acryloyl)-5-methoxyphenyl)-benzamide (10). The title compound was synthesized from **2** and 3-bromobenzoyl chloride to yield a yellow solid (49 %).

(*E*)-*N*-(2-(3-(3,4-dimethoxyphenyl)acryloyl)-5-methoxyphenyl)-2-methoxybenzamide (11). The title compound was synthesized from **2** and 2-methoxybenzoyl chloride to yield a yellow solid (42 %).

(*E*)-*N*-(2-(3-(3,4-dimethoxyphenyl)acryloyl)-5-methoxyphenyl)nicotinamide (12). The title compound was synthesized from **2** and nicotinoyl chloride to yield a yellow solid (27 %).

(*E*)-*N*-(2-(3-(3,4-dimethoxyphenyl)acryloyl)-5-methoxyphenyl)picolinamide (13). The title compound was synthesized from **2** and picolinoyl chloride to yield a yellow solid (22 %).

(*E*)-*N*-(2-(3-(3,4-dimethoxyphenyl)acryloyl)-5-methoxyphenyl)-1-naphthamide (14). The title compound was synthesized from **2** and 1-naphthoyl chloride to yield a yellow solid (32 %).

(*E*)-*N*-(2-(3-(3,4-dimethoxyphenyl)acryloyl)-5-methoxyphenyl)quinoline-3-carboxamide (15). The title compound was synthesized from **2** and quinolone-3-carbonyl chloride to yield a yellow solid (30 %).

(*E*)-*N*-(2-(3-(3,4-dimethoxyphenyl)acryloyl)-5-methoxyphenyl)thiophene-2-carboxamide (16). The title compound was synthesized from **2** and thiophene-2-carbonyl chloride to yield a yellow solid (51 %).

(*E*)-*N*-(2-(3-(3,4-dimethoxyphenyl)acryloyl)-5-methoxyphenyl)furan-2-carboxamide (17). The title compound was synthesized from **2** and 2-furoyl chloride to yield a pale-yellow solid (46 %).

(*E*)-*N*-(2-(3-(3,4-dimethoxyphenyl)acryloyl)-5-methoxyphenyl)thiazole-2-carboxamide (18). The title compound was synthesized from **2** and thiazole-2-carbonyl chloride to yield a yellow solid (72 %).

(*E*)-*N*-(2-(3-(3,5-dimethoxyphenyl)acryloyl)-5-methoxyphenyl)benzamide (19). The title compound was synthesized from **3** and benzoyl chloride to yield a yellow solid (41 %).

(*E*)-*N*-(2-(3-(3,5-dimethoxyphenyl)acryloyl)-5-methoxyphenyl)-2-methoxybenzamide (20). The title compound was synthesized from **3** and 2-methoxybenzoyl chloride to yield a yellow solid (30 %).

(*E*)-2-chloro-*N*-(2-(3-(3,5-dimethoxyphenyl)acryloyl)-5-methoxyphenyl)benzamide (21). The title compound was synthesized from **3** and 2-chlorobenzoyl chloride to yield a yellow solid (34 %).

(*E*)-*N*-(2-(3-(3,5-dimethoxyphenyl)acryloyl)-5-methoxyphenyl)thiophene-2-carboxamide (22). The title compound was synthesized from **3** and thiophene-2-carbonyl chloride to yield a yellow solid (74 %).

(*E*)-*N*-(2-(3-(3,5-dimethoxyphenyl)acryloyl)-5-methoxyphenyl)-1-naphthamide (23). The title compound was synthesized from **3** and 1-naphthoyl chloride to yield a yellow solid (53 %).

(*E*)-*N*-(2-(3-(3,4-dimethoxyphenyl)acryloyl)-4,5-dimethoxyphenyl)benzamide (24). The title compound was synthesized from **4** and benzoyl chloride to yield a yellow solid (79 %).

(*E*)-*N*-(2-(3-(3,4-dimethoxyphenyl)acryloyl)-4,5-dimethoxyphenyl)-2-methoxybenzamide (25). The title compound was synthesized from **4** and 2-methoxybenzoyl chloride to yield a yellow solid (89 %).

(*E*)-*N*-(2-(3-(3,4-dimethoxyphenyl)acryloyl)-4,5-dimethoxyphenyl)thiophen-2-carboxamide (26). The title compound was synthesized from **4** and thiophene-2-carbonyl chloride to yield pale orange solid (57 %).

(*E*)-2-(3-(3,4-dimethoxyphenyl)acryloyl)-5-methoxyphenyl benzoate (27). The title compound was synthesized from **5** and benzoylchloride to yield a yellow solid (60 %).

(*E*)-2-(3-(3,4-dimethoxyphenyl)acryloyl)-5-methoxyphenyl thiophene-2-carboxylate (28). The title compound was synthesized from **5** and thiophene-2-carbonyl chloride to yield a yellow solid (57 %).

(*E*)-2-(3-(3,4-dimethoxyphenyl)acryloyl)-5-methoxyphenyl 2-methoxybenzoate (29). The title compound was synthesized from **5** and 2-methoxybenzoyl chloride to yield a yellow solid (53 %).

(*E*)-2-(3-(3,5-dimethoxyphenyl)acryloyl)-5-methoxyphenyl benzoate (30). The title compound was synthesized from **6** and benzoylchloride to yield a yellow solid (70 %).

(*E*)-2-(3-(3,5-dimethoxyphenyl)acryloyl)-5-methoxyphenyl thiophene-2-carboxylate (31). The title compound was synthesized from **6** and thiophene-2-carbonyl chloride to yield a yellow solid (62 %).

(*E*)-2-(3-(3,5-dimethoxyphenyl)acryloyl)-5-methoxyphenyl 2-methoxybenzoate (32). The title compound was synthesized from **6** and 2-methoxybenzoyl chloride to yield a yellow solid (66 %).

Biological investigations

Chemicals: The reference compounds cyclosporine A and Ko143 were purchased from Tocris Bioscience (Bristol, UK). Calcein AM, the non-fluorescent acetomethoxy ester derivative of calcein, was delivered by Merck KGaA (Darmstadt, Germany). Cell culture material was supplied by Sarstedt (Newton, USA), and all other chemicals were purchased from Sigma–Aldrich (Taufkirchen, Germany) unless otherwise specified.

Cell culture: MDCK II BCRP and MDCK II wild-type cell lines were received as a generous gift from Dr. A. Schinkel (The Netherlands Cancer Institute, Amsterdam, The Netherlands). Cells were generated by transfection of the canine kidney epithelial cell line MDCK II with the human wild-type cDNA of ABCG2 C-terminally linked to the cDNA of the green fluorescent protein (GFP). MDCK II cells

were cultured in Dulbecco's modified Eagle's medium (DMEM) supplemented with 10% fetal calf serum (FCS), 50 μg mL^{-1} streptomycin, 50 U mL^{-1} penicillin G, and 2 mm L-glutamine. The doxorubicin-resistant human ovarian carcinoma cell line A2780adr was further used for calcein AM assays. This ABCB1-overexpressing cell line was purchased from the European collection of animal cell cultures (ECACC, 93112520, UK) and cultured in RPMI-1640 medium, supplemented with 10% FCS, 50 μg mL^{-1} streptomycin, 50 U mL^{-1} penicillin G, and 2 mm L-glutamine. H69 AR, the small-cell lung cancer cell line, expressing ABCC1 (multidrug resistance-associated protein 1) was obtained from American Type Culture Collection (ATCC, CRL-11351). These cells were grown in RPMI-1640 medium with 20% FCS, 50 μg mL^{-1} streptomycin, 50 U mL^{-1} penicillin G, and 2 mm L-glutamine. Cell lines were incubated in a 5% CO_2 humidified atmosphere at 37 °C and harvested for sub-culturing with 0.05% trypsin and 0.02% EDTA.

Hoechst 33342 accumulation assays: To analyze the inhibitory effect of title compounds on ABCG2, the Hoechst 33342 accumulation assay was performed as described earlier with small modifications.[24,30,35] Various dilutions of each compound were prepared in Krebs-Hepes buffer (KHB). The highest concentrations (10 μm) were prepared from a 10^{-2} m stock solution in DMSO, methanol, and KHB. A volume of 20 μL from each dilution was placed into black 96-well plates (Greiner, Frickenhausen, Germany). For further preparation, cells were harvested after reaching a confluence of 80–90% by gentle trypsination (0.05% trypsin/0.02% EDTA). Following the addition of culture medium, cells were transferred into 50 mL tubes and centrifuged (266 g, 4 °C; 4 min). Obtained cell pellets were resuspended in fresh culture medium and cells were counted using a CASY1 model TT cell counter device (Schaerfe System GmbH, Reutlingen, Germany). After three washing steps with KHB by centrifugation, ~30 000 cells per well were placed in a volume of 160 μL. In all assays the highest concentration of DMSO was not > 0.1% and of methanol not > 4%. The plates were incubated for 30 min under 5% CO_2 at 37 °C. Furthermore 20 μL of a 10 μm Hoechst 33342 solution (protected from light) was placed in each well and the fluorescence was measured at constant time intervals (60 s) for a period of 120 min at an excitation wavelength of 355 nm and an emission wavelength of 460 nm at 37 °C. For measurement a BMG POLARstar microplate reader (BMG Labtech, Offenburg, Germany) was used. The average of fluorescence values in the steady state (100–109 min) was calculated for all concentrations. From these data concentration–response curves were generated by nonlinear regression using the three- or four-parameter logistic equation, whichever was statistically preferred (GraphPad Prism, version 5.0, San Diego, CA, USA). From the pIC$_{50}$ values and their standard deviations, IC$_{50}$ values and standard deviations were calculated according to the equation for log-normal distributed values.[43,44]

Calcein AM assays: To evaluate the compounds for their selectivity toward ABCB1 and ABCC1 inhibition, calcein AM assays were performed as described previously with minor modifications.[28,30,32] The procedure for dilution series and preparation of cell suspension was identical to the Hoechst 33342 assay. The dilution series were pipetted into colorless 96-well plates (Greiner, Frickenhausen, Germany) in a volume of 20 μL. A2780adr cells for ABCB1 and H69 AR cells for ABCC1 were then placed into the plates at a density of ~30 000 cells per well to reach a total volume of 180 μL. Following a 30 min pre-incubation under 5% CO_2 at 37 °C, 20 μL of a 3.125 μm calcein AM solution (protected from light) was added to each well. Immediately, the fluorescence was measured at constant time intervals (60 s) for a period of 60 min at 37 °C at an exci-

tation wavelength of 485 nm and an emission wavelength of 520 nm. For measurement the BMG POLARstar microplate reader (BMG Labtech, Offenburg, Germany) was used. From the pIC$_{50}$ values and their standard deviations, IC$_{50}$ values and standard deviations were calculated according to the equation for log-normal distributed values.[43,44]

MTT assays for determining cytotoxicity: Intrinsic cytotoxicity of selected compounds was analyzed by MTT colorimetric assay using MDCK II BCRP and MDCK II wild-type cells.[28,33] Based on mitochondrial dehydrogenases of viable cells MTT is reduced to purple formazan, which is quantified spectrophotometrically. The assay was performed as described previously with minor modifications. Cells were harvested as described above and seeded into 96-well tissue-culture treated plates (Starlab GmbH, Hamburg, Germany) at a density of ~3000 cells per well in a total volume of 180 μL. The plates were kept under 5% CO_2 atmosphere and 37 °C for 6 h, for attachment of cells. Various concentrations of selected compounds were prepared in culture medium. Then 20 μL of each dilution was added to reach the final concentration in a volume of 200 μL. The highest concentration of DMSO used in the assay was not > 0.1% and of methanol not > 4%. Furthermore, two wells per row were prepared with either 10% (v/v) DMSO (positive control) or pure culture medium (negative control). For reducing the evaporation of solvent during the incubation time of 72 h, phosphate-buffered saline (PBS) was added to the interspaces of the plates. After three days a solution of MTT (3-(4,5-dimethylthiazole-2-yl)-2,5-diphenyltetrazolium bromide) in PBS (5 mg mL^{-1}) was added to each well in a volume of 20 μL. During the incubation of 1 h, MTT is reduced to purple formazan. The liquid was removed to stop the reaction and the cells were lysed by adding 100 μL DMSO to each well. Absorbance was measured at 570 nm and background correction at 690 nm using a Multiscan Ex microplate photometer (Thermo Fisher Scientific, Waltham, MA, USA). The obtained data sets were normalized, and GI$_{50}$ values calculated by nonlinear regression analysis, assuming a sigmoidal concentration–response curve with variable Hill slope (GraphPad Prism, version 5.0, San Diego, CA, USA).

MTT assay for determining the ability of MDR reversal: Besides the detection of cytotoxicity, the MTT assay was also used to evaluate the effect of inhibitors on the reversal of resistance against cytotoxic compounds like SN-38 (active metabolite of irinotecan). For this purpose, the cytotoxic effect of SN-38 in the absence or presence of various concentrations of selected inhibitors was measured. MDCK II wild-type and MDCK II BCRP cells were seeded into 96-well tissue-culture treated plates in a total volume of 160 μL with a density of ~3000 cells per well. Subsequently plates were incubated under 5% CO_2 atmosphere and 37 °C for 6 h. From previously prepared dilution series of SN-38 in culture medium, 20 μL of each concentration was added to the cell containing wells. Afterward 20 μL of culture medium (negative control) as well as 1 and 5 μm test compound were added to the wells containing MDCK II BCRP cells. Thereby was accomplished the final concentration in a total volume of 200 μL. As positive control, 20 μL of culture medium was added to the MDCK II wild-type cells. The subsequent steps were performed as described above. From the pIC$_{50}$ values and their standard deviations, IC$_{50}$ values and standard deviations were calculated according to the equation for log-normal distributed values.[43,44]

ATPase assays: ATPase activity was measured as described previously with slight modifications by a sensitive colorimetric detection of inorganic phosphate.[35] The isolated Sf9 cell membranes were obtained after three days infection with a recombinant baculovirus

↖↖ **These are not the final page numbers!**

with the human wild-type ABCG2 cDNA and a cholesterol-loading step membrane preparation, as described.[12,45,46] The membrane suspensions (10 μg of the prepared membrane protein) were incubated in assay mixture containing 40 mm 3-(N-morpholino)propanesulfonic acid-Tris (pH 7.0), 50 mm KCl, 2 mm dithiothreitol, 0.5 mm EGTA-Tris (pH 7.0), 5 mm sodium azide, 1 mm ouabain. The test compounds were added in DMSO. The final DMSO concentration was <1%, and had no effect on ATPase activity. The reaction was started by adding 10 μL of 50 mm Mg·ATP. The incubation time was 20 min at 37°C. After stopping the reaction by addition of 5% sodium dodecyl sulfate (SDS), the samples were supplemented with the Pi reagent (containing 2.5 m H_2SO_4, 1% ammonium molybdate, 0.014% antimony potassium tartrate), 20% acetic acid and 1% freshly prepared ascorbic acid. The optical density was measured at a wavelength of 880 nm. The calibration line was determined with K_2HPO_4 and was used for determination the amount of phosphate from the absorbance values.

Molecular modeling

Molecular modeling was performed with MOE 2014.09.[47] The compounds were built and energy minimized using the MMFF94x force field. Then a conformational search was performed by applying the low-mode MD algorithm with standard settings. The low-mode MD search algorithm generates conformations using a short ~1 ps run of molecular dynamics at constant temperature (300 K) followed by an all-atom energy minimization. Initially intended for large, possibly disconnected, and complex structures like macrocycles and protein loops, the method is also very efficient for detailed small-molecule analysis. The key to the efficiency of the method lies in the specification of the initial MD velocities: random kinetic energy is given mainly on the low-frequency vibrational modes of the molecular system causing rapid and more realistic conformational transitions. The resulting conformations are saved to the output database provided they meet the energetic and geometric criteria. Ten conformations with lowest energy were visually inspected and found to be very similar in shape in both cases. Therefore, the conformations with lowest energy were selected and superimposed. For comparison a flexible alignment of both compounds (**7** and **27**) was performed and the potential energies calculated.

Notes

This manuscript was written through contributions of all authors. All authors have given approval to the final version of the manuscript. The authors declare no competing financial interest.

Abbreviations

ABC, ATP binding cassette; BCRP, breast cancer resistance protein (ABCG2); MDCK, Madin–Darby canine kidney; CsA, cyclosporine A; FTC, fumitremorgin C; I_{max}, maximal inhibition; GI_{50}, half-maximal growth inhibition.

Acknowledgements

[1] R. J. Kathawala, P. Gupta, C. R. Ashby, Jr., Z.-S. Chen, *Drug Resist. Updates* **2015**, *18*, 1–17.
[2] M. M. Gottesmann, *Annu. Rev. Med.* **2002**, *53*, 615–627.
[3] C. F. Higgins, *Annu. Rev. Cell Biol.* **1992**, *8*, 67–113.
[4] E. Dassa, P. Bouige, *Res. Microbiol.* **2001**, *152*, 211–229.
[5] *ABC Proteins* (Eds: I. B. Holland, S. P. C. Cole, K. Kuchler, C. F. Higgins), Academic Press, London, UK, **2003**.
[6] C. P. Wu, C. H. Hsieh, Y. S. Wu, *Mol. Pharm.* **2011**, *8*, 1996–2011.
[7] G. Szakács, J. K. Paterson, J. A. Ludwig, C. Booth-Genthe, M. M. Gottesmann, *Nat. Rev. Drug Discovery* **2006**, *5*, 219–234.
[8] J. A. Endicott, V. Ling, *Annu. Rev. Biochem.* **1989**, *58*, 137–171.
[9] S. P. C. Cole, G. Bhardwaj, J. H. Gerlach, J. E. Mackie, C. E. Grant, K. C. Almquist, A. J. Stewart, E. U. Kurz, A. M. V. Duncan, R. G. Deeley, *Science* **1992**, *258*, 1650–1654.
[10] L. A. Doyle, W. Yang, L. V. Abruzzo, T. Krogmann, Y. Gao, A. K. Rishi, D. D. Ross, *Proc. Natl. Acad. Sci. USA* **1998**, *95*, 15665–15670.
[11] L. A. Doyle, D. D. Ross, *Oncogene* **2003**, *22*, 7340–7358.
[12] C. Özvegy, T. Litman, G. Szakács, Z. Nagy, S. Bates, A. Váŕadi, B. Sarkadi, *Biochem. Biophys. Res. Commun.* **2001**, *285*, 111–117.
[13] H. Wang, E. W. Lee, X. Cai, Z. Ni, L. Zhou, Q. Mao, *Biochemistry* **2008**, *47*, 13778–13787.
[14] K. Wong, S. J. Briddon, N. D. Holliday, I. D. Kerr, *Biochim. Biophys. Acta Mol. Cell Res.* **2016**, *1863*, 19–29.
[15] K. Natarajan, Y. Xie, M. R. Baer, D. D. Ross, *Biochem. Pharmacol.* **2012**, *83*, 1084–1103.
[16] T. Litman, M. Brangi, E. Hudson, P. Fetsch, P. Abati, D. D. Ross, K. Miyake, J. H. Resau, S. Bates, *J. Cell Sci.* **2000**, *113*, 2011–2021.
[17] S. Rabindran, H. He, M. Singh, E. Brown, K. Collins, T. Annable, L. Greenberger, *Cancer Res.* **1998**, *58*, 5850–5858.
[18] S. Rabindran, D. Ross, L. Doyle, W. Yang, L. Greenberger, *Cancer Res.* **2000**, *60*, 47–50.
[19] M. Nishiyama, T. Kuga, *Jpn. J. Pharmacol.* **1989**, *50*, 167–173.
[20] J. D. Allen, A. van Loevezijn, J. M. Lakhai, M. van der Valk, O. van Tellingen, G. Reid, J. H. M. Schellens, G. J. Koomen, A. H. Schinkel, *Mol. Cancer Ther.* **2002**, *1*, 417–425.
[21] A. van Loevezijn, J. D. Allen, A. H. Schinkel, G. J. Koomen, *Bioorg. Med. Chem. Lett.* **2001**, *11*, 29–32.
[22] F. Lecerf-Schmidt, B. Peres, G. Valdameri, C. Gauthier, E. Winter, L. Payen, A. Di Pietro, A. Boumendjel, *Future Med. Chem.* **2013**, *5*, 1037–1045.
[23] K. Juvale, V. F. Pape, M. Wiese, *Bioorg. Med. Chem.* **2012**, *20*, 346–355.
[24] K. Juvale, J. Gallus, M. Wiese, *Bioorg. Med. Chem.* **2013**, *21*, 7858–7873.
[25] S. Kraege, S. C. Köhler, M. Wiese, *ChemMedChem* **2016**, DOI: 10.1002/cmdc.201600341.
[26] G. H. Jin, S. K. Ha, H. M. Park, B. Kang, S. Y. Kim, H.-D. Kim, J.-H. Ryu, R. Jeon, *Bioorg. Med. Chem. Lett.* **2008**, *18*, 4092–4094.
[27] M. Kim, H. Turnquist, J. Jackson, M. Sgagias, Y. Yan, M. Gong, M. Dean, J. G. Sharp, K. Cowan, *Clin. Cancer Res.* **2002**, *8*, 22–28.
[28] F. Marighetti, K. Steggemann, M. Hanl, M. Wiese, *ChemMedChem* **2013**, *8*, 125–135.
[29] J. Gallus, K. Juvale, M. Wiese, *Biochim. Biophys. Acta Biomembr.* **2014**, *1838*, 2929–2938.
[30] A. Pick, W. Klinkhammer, M. Wiese, *ChemMedChem* **2010**, *5*, 1498–1505.
[31] P. Labute, *J. Chem. Inf. Model.* **2010**, *50*, 792–800.
[32] S. Köhler, M. Wiese, *J. Med. Chem.* **2015**, *58*, 3910–3921.
[33] H. Mueller, M. U. Kassack, M. Wiese, *J. Biomol. Screening* **2004**, *9*, 506–515.
[34] A. Seelig, *Eur. J. Biochem.* **1998**, *251*, 252–261.
[35] S. Kraege, K. Stefan, K. Juvale, T. Ross, T. Willmes, M. Wiese, *Eur. J. Med. Chem.* **2016**, *117*, 212–229.
[36] R. Badhan, J. Penny, *Eur. J. Med. Chem.* **2006**, *41*, 285–295.
[37] J. Boccard, F. Bajot, A. Di Pietro, S. Rudaz, A. Boumendjel, E. Nicolle, P.-A. Carrupt, *Eur. J. Pharm. Sci.* **2009**, *36*, 254–264.

These are not the final page numbers! ↗↗

[38] G. Kothandan, C. G. Gadhe, T. Madhavan, C. H. Choi, S. J. Cho, *Eur. J. Med. Chem.* **2011**, *46*, 4078–4088.

[39] F. Bois, C. Beney, A. Boumendjel, A. M. Mariotte, G. Conseil, A. Di Pietro, *J. Med. Chem.* **1998**, *41*, 4161–4164.

[40] F. Bois, A. Boumendjel, A. M. Mariotte, G. Conseil, A. Di Petro, *Bioorg. Med. Chem.* **1999**, *7*, 2691–2695.

[41] E. B. Yang, K. Zhang, L. Y. Cheng, P. Mack, *Biochem. Biophys. Res. Commun.* **1998**, *245*, 435–438.

[42] E. B. Yang, Y. J. Guo, K. Zhang, Y. Z. Chen, P. Mack, *Biochim. Biophys. Acta Protein Struct. Mol. Enzymol.* **2001**, *1550*, 144–152.

[43] *Log-normal distribution*, Wikipedia: https://en.wikipedia.org/wiki/Log-normal_distribution (last accessed October 3, 2016).

[44] MathWorks: http://de.mathworks.com/help/stats/lognstat.html (last accessed October 3, 2016).

[45] A. Telbisz, M. Müller, C. Özvegy-Laczka, L. Homolya, L. Szente, A. Varadi, B. Sarkadi, *Biochim. Biophys. Acta Biomembr.* **2007**, *1768*, 2698–2713.

[46] B. Sarkadi, A. Telbisz (Cellpharma LLC), WO2013128217 A1, **2013**.

[47] Chemical Computing Group, 1010 Sherbrooke St. West, Suite 910, Montreal, QC, H3A 2R7 (Canada).

↖↖ **These are not the final page numbers!**

FULL PAPERS

Efflux pump deactivators: Methoxy-substituted acryloylphenylcarboxamides are a class of highly potent inhibitors of the ATP binding cassette G2 (ABCG2). A comparison with acryloylphenylcarboxylates highlighted the beneficial effect of an amide function for inhibitory activity toward this drug efflux pump, which plays a role in multidrug resistance.

Structural features of acryloylphenylcarboxamides
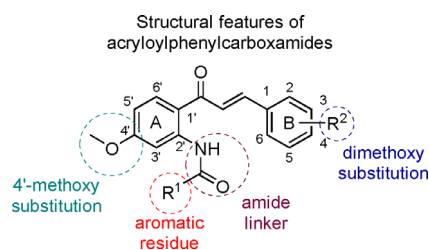
S. Kraege, K. Stefan, S. C. Köhler, M. Wiese*

■■ – ■■

Optimization of Acryloylphenylcarboxamides as Inhibitors of ABCG2 and Comparison with Acryloylphenylcarboxylates

These are not the final page numbers! ↗↗